Front. Earth Sci.
DOI 10.1007/s11707-016-0632-x

RESEARCH ARTICLE

Sediment transport in headwaters of a volcanic catchment—Kamchatka Peninsula case study

Sergey R. CHALOV (✉)[1], Anatolii S. TSYPLENKOV[1], Jan PIETRON[2], Aleksandra S. CHALOVA[1], Danila I. SHKOLNYI[1], Jerker JARSJÖ[2], Michael MAERKER[3]

1 Faculty of Geography, M. V. Lomonosov Moscow State University, Moscow 119911, Russia
2 Department of Physical Geography and the Bolin Centre for Climate Research, Stockholm University, Stockholm 10691, Sweden
3 Department of Earth and Environmental Sciences, Pavia University, Pavia 27100, Italy

Abstract Due to specific environmental conditions, headwater catchments located on volcanic slopes and valleys are characterized by distinctive hydrology and sediment transport patterns. However, lack of sufficient monitoring causes that the governing processes and patterns in these areas are rarely well understood. In this study, spatiotemporal water discharge and sediment transport from upstream sources was investigated in one of the numerous headwater catchments located in the lahar valleys of the Kamchatka Peninsula Sukhaya Elizovskaya River near Avachinskii and Koryakskii volcanoes. Three different subcatchments and corresponding channel types (wandering rivers within lahar valleys, mountain rivers within volcanic slopes and rivers within submountain terrains) were identified in the studied area. Our measurements from different periods of observations between years 2012–2014 showed that the studied catchment was characterized by extreme diurnal fluctuation of water discharges and sediment loads that were influenced by snowmelt patterns and high infiltration rates of the easily erodible lahar deposits. The highest recorded sediment loads were up to $9 \cdot 10^4$ mg/L which was related to an increase of two orders of magnitude within a one day of observations. Additionally, to get a quantitative estimate of the spatial distribution of the eroded material in the volcanic substrates we applied an empirical soil erosion and sediment yield model – modified universal soil loss equation (MUSLE). The modeling results showed that even if the applications of the universal erosion model to different non-agricultural areas (e.g., volcanic catchments) can lead to irrelevant results, the MUSLE model delivered might be acceptable for non-lahar areas of the studied volcanic catchment. Overall the results of our study increase our understanding of the hydrology and associated sediment transport for prediction of risk management within headwater volcanic catchments.

Keywords sediment transport, volcanoes, lahars, Kamchatka Peninsula, MUSLE, erosion

Received September 5, 2016; accepted November 30, 2016

E-mail: srchalov@geogr.msu.ru

1 Introduction

Volcanic environments are associated with the highest known sediment yields and erosion rates (Smith and Lowe, 1991; Manville et al., 2000; Eiriksdottir et al., 2008; Thouret et al., 2014). It is because of an abundance of loose, granular material stored on poorly vegetated, steep slopes of the volcanic river basins (Oguchi et al., 2001; Hayes et al., 2002). The observed sediment flows in volcanic environments range from lower concentrated stream-flows (Mouri et al., 2014) to hyperconcentrated and debris flows (Doyle et al., 2011). However, due to high infiltration potential of young volcanic rocks and sediments, regular stream-flows often occur episodically (Rad et al., 2007; Mouri et al., 2014). The hyperconcentrated and debris flow events, commonly termed "lahars", are related to a rapidly flowing mixture of water and volcanic rocks (Smith and Fritz, 1989). The most catastrophic lahars are triggered by a rapid melt of snow and ice cups or breakthrough of a crater lake during eruption events (Lavigne et al., 2000). Loose pyroclastic material remaining in the primary lahar source or deposited in stream channels after syn-eruptive lahar, can be still subject to erosion. Thus, heavy rainfall events or snow melts due to warm air temperature can easily trigger secondary, post-eruptive lahars and mudflows (Rodolfo and Arguden, 1991; Cronin et al., 1999; Tanarro et al., 2010).

Lahar deposits were found to act as long term supply of volcanic material that increase sediment yields of

rainfall-runoff events (Major et al., 2000; Oguchi et al., 2001; Hayes et al., 2002; Gran and Montgomery, 2005). Additionally, as shown by Mouri et al. (2014) sediment flow events related to air temperature-triggered snow melt on lahar valleys can significantly increase sediment concentrations during regular flow events. However, the water and sediment supply during rainfall and snow melt events may have a highly irregular character due to factors such as: (i) varying temporal (seasonal, daily, and hourly) regime of snowmelt (Hock, 1999; Pellerin et al., 2012), (ii) spatiotemporal variability of melt water retention of snow packs (Gerdel, 1954; Bøggild, 2000) and (iii) high permeability of mouldy volcanic rocks (Mouri et al., 2014).

Kamchatka Peninsula is one of the largest volcanic areas of the world (472.300 km^2) which is situated in the far east of Russia, between the Sea of Okhotsk and the Pacific Ocean. High volcanic activity characterized by 70 active volcanoes in Holocene covered large parts of the peninsula with Holocene and Pleistocene volcanic debris and lahar deposits (Ponomareva et al., 2007). Due to the specific geology of the volcanic slopes headwater streams called "dry rivers" have an irregular, spatiotemporal character. Lack of monitoring stations (Kuksina and Chalov, 2012) hinders the understanding of the water discharge and sediment transport dynamics in the volcanic headwater catchments of Kamchatka Peninsula.

This study presents field observations (water discharge and sediment load) from different locations within a small volcanic headwater catchment of 25 km^2 size in order to get a detailed insight about the spatiotemporal runoff and erosion dynamics triggered by precipitation and snowmelt events. Furthermore, we applied an empirical modeling approach (MUSLE) and estimated the sediment delivery ratio (SDR) taking into account the heterogeneity of the landscape in terms of vegetation and topography. As already stated by several authors the USLE approach was mainly made for the assessment of agricultural areas (e.g., Wischmeier and Smith, 1978; Boardman, 1996; Renard et al., 1997). Therefore, the application of models to different environments is often inappropriate. Nonetheless, it is often the only approach to get a first idea about the relative distribution of erosion intensities since the input data is relatively easy to derive. Hence, we apply here the MUSLE in volcanic substrates to get a first rough quantitative estimate of the spatial distribution of eroded sediments.

2 Materials and methods

2.1 Site description

The study area is drained by the Sukhaya Elizovskaya River and its tributaries. The River system is one of the numerous headwater drainages located in the lahar valleys of the Kamchatka Peninsula (Figs. 1). The Sukhaya Elizovskaya has an ephemeral character. It drains only during large floods (Fig. 1(b)) into the Mutnaya River that tin turn is a tributary of the Avacha River located in the basin of the Avachinsky Bay, Pacific Ocean. Total length of the Sukhaya Elizovskaya River is about 20 km and its basin area is almost 174 km^2 (Fig. 1(c)). The river has two constant and several temporal tributaries and located on the slopes of the Avachinskii and Koryakskii volcanoes (Marenina et al., 1962). The river catchment is located in a southeast soil province (a zone of stone birch forests) where the prevailing soil type is volcanic, generated on volcanic ashes that accumulated after the eruption of Avachinskii volcano in 1926 (Chernomorets and Seynova, 2010).

The Sukhaya Elizovskaya River basin is characterized by a high spatial and temporal variability of the snow cover (Fig. 2). According to our analysis of satellite images from the 28th of May, 15th of July and the 1st of September 2013 (the normalized snow index NDSI based on Landsat 7 ETM; Fig. 2 and Fig. 3) about 80% of the basin area was covered by snow in late May. The percentage of the basin area covered by snow decreases to 24% and 15% in mid-July and beginning of September respectively. Hence, the snowmelt runoff formation can occur during a period between May and end of July.

The climate of the Sukhaya Elizovskaya River basin is characterized by huge daily and seasonal temperature fluctuations. According to Elizovo meteostation the average annual temperature is 1.9°C (2005–2015) with average monthly maximum and minimum temperatures in August of 15.3°C and in January of –10.5°C, respectively. The average annual precipitation for the basin for last ten years (2005–2015) was 986 mm. Most of the annual precipitation occurs as snowfall events during the autumn and winter months (October–March). The record maximum daily precipitation (182 mm in both the liquid and solid forms) was registered in the 23rd of November 1995. The absolute maximum monthly precipitations were registered in December 2010 with 346 mm and in October 2012 with 415 mm (Fig. 3).

Different landscapes of volcanic, tectonic and glacial origins determine the variability of the channel types in the mountainous and plain areas of the Kamchatka Peninsula (Ermakova, 2008). The combination of variables that discriminates specific channel patterns mostly represent a dominant factor in the evolution of river valley geomorphology and relates to river types (mountain, semi-mountain, and plain) and conditions of channels development (incised, confined or wide floodplain channels) (Alexeevsky et al., 2013). The eastern parts of the peninsula (East Volcanic Geomorphological Area), where Sukhaya Elizovskaya River basin is located, dominate in mountain channels of lahar valleys, meandering mountain channels and meandering semi-mountain channels (Chalov et al., 2014).

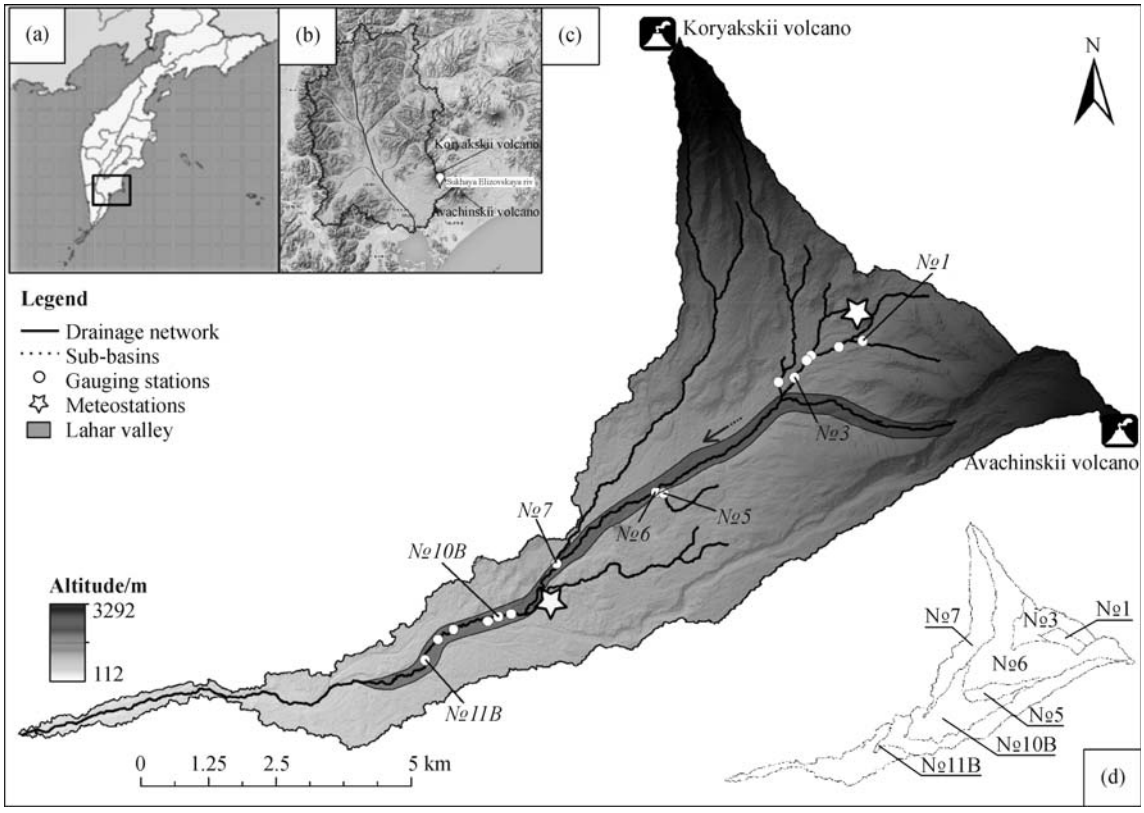

Fig. 1 Location of gauging stations in the studied catchment.

The fluvial system of the Sukhaya Elizovskaya River was generated within ancient lahar deposits originating from the Avachinskii volcano and a flat detrital cone in the form of inclined alluvial of an apron (so-called lahar valley). The profile of the river basin, which flattened out longitudinally, is very sharp (from 60 ‰–70 ‰ to 15 ‰–20 ‰). Such terrain determines the variability of channel patterns and unique conditions of sediment transport. Generally, the Sukhaya Elizovskaya basin can be divided into three different types of watersheds (sub-catchments) related to channel patterns, vegetation types, topography and snow cover occurrence and distribution modes (Chalov et al., 2014):

I- the watersheds covering steep volcanic slopes characterized with an open and easily eroded surface. River channels are characterized by mainly coarse material;

II- the watersheds covering parts of lahar valleys composed of tuff conglomerates and conglobreccia deposits. Channels are formed in a mass of easily eroded depositions that defines it wandering and formation of braided channel.

III- the watersheds located within submountain terrains of an average steepness with shrub vegetation on old volcanic depositions and diffused coarse material within river valleys.

2.2 Hydrological data acquisition and processing

Field data have been acquired during several field covering different hydrological seasons: (i) spring flood with an intensive snow melting at the downstream part of the catchment and rainfalls (May 2007), (ii) summer low water period with rainfalls and snow melting at the upper part of the catchment (end of July–August 2012, June 2013, and June 2014). Hydrological measurements were carried out at maximum 12 gauging stations along the river and its tributaries (white points, Fig. 1) from 4 to 12 times per day depending on the hydrological conditions during the campaigns. Stations from No 1 to No 3 were located in the steep channels on volcanoes slopes covering watershed type I. Stations No 6, No 10B and No 11B were located in the lahar streams of watershed type II. The remaining stations No 5 and No 7 were located in the tributaries of the Sukhaya Elizovskaya River in the mountain channels of watershed types III. In August 2012 and June 2014 the measurements were done mainly in the upper part of the basin, whereas in 2013 the measurements covered the middle and downstream parts.

Flow velocity measurements were done using propeller type current meters at flow depth 0.6h (where h is the flow depth in meters). The water discharge was calculated by

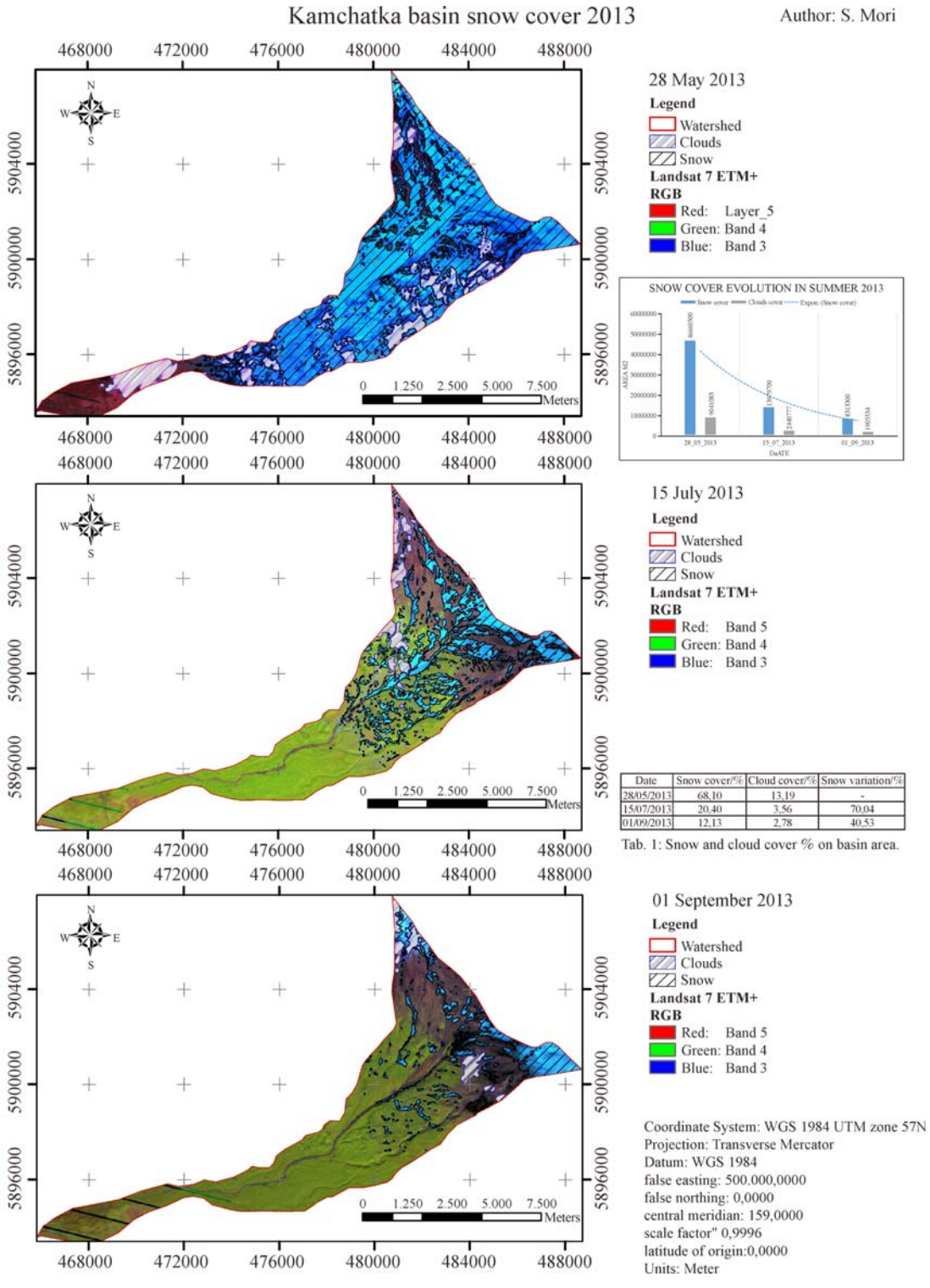

Date	Snow cover/%	Cloud cover/%	Snow variation/%
28/05/2013	68,10	13,19	-
15/07/2013	20,40	3,56	70,04
01/09/2013	12,13	2,78	40,53

Tab. 1: Snow and cloud cover % on basin area.

Fig. 2 Snow cover variability during flow observations in 2013.

multiplying watercourse cross sectional area (m^2) by the flow velocity (m/s). The suspended sediment concentration (*SSC*) was measured using a portable optical turbidity meter HACH 2100P (water turbidity, NTU) and by filtering method (*SSC*, g/m^3) which also considered relatively coarse sediments (sand and gravel). The latter were found in suspension under flow increase because of low weights of pyroclastic material. For the fine particles relationship between (SSC and NTU ($R^2 = 0.92$) was built to further recalculation of optical values (NTU) to concentration units (g/m^3).

Meteorological parameters (air temperature, °C; pre-

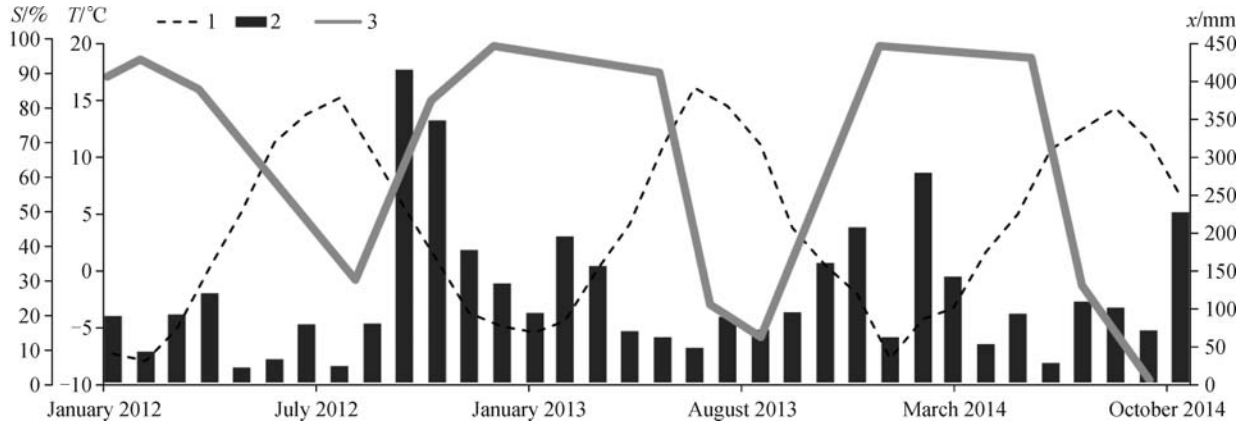

Fig. 3 Temporal changes of temperature (1), precipitation (2) and snow cover (3) within Sukhaya Elizovskaya river in 2012–2014.

cipitation, mm) were registered by two automatic meteostations Davis Vantage Pro II. The location of these stations are shown in Fig. 1(c). The correlation between Elizovo measurements and field observations, made during field seasons 2012–2014 is rather high ($r = 0.7$). Therefore we consider the data of the meteorological station of Elizovo representative for the entire basin. All model calculations and mapping were made in ArcMap 10.2.2. A GIS project was set up including different vector layers (river network, watersheds), satellite images (Landsats 7 ETM +, 8), digital elevation model (DEM) ALOS WORLD 3D and model input and output raster layers.

The ALOS WORLD 3D DEM is a 5 m DEM generated from ALOS PRISM data. The ALOS World 3D Topographic Data product, known as AW3D, is currently being produced by Japanese companies RESTEC/NTT Data. AW3D uses the extensive archive stereo coverage that was collected by ALOS PRISM during the period 2005–2011. The original data usually is a bit roughly, hence the DEM preprocessing and hydrology correction were made in open-source SAGA GIS. First of all a mesh denoising (Sun et al., 2007) was made and then filling of surface depressions (Wang and Liu, 2006). Other operations such as flow accumulation, direction, slope, etc. were made using Spatial Analyst tools in ArcMap 10.2.2.

2.3 Soil Erosion Modeling

2.3.1 MUSLE approach

To study variability of the erosion patterns during the different hydrological seasons we compiled field observations with a spatial distribution modeling approach, Modified Universal Soil Loss Equation (MUSLE; Williams, 1975) (modification of standard USLE (Universal Soil Loss Equation; Wischmeier and Smith, 1960)):

$$Y = 11.8 \cdot (Q_T \cdot Q_{\max})^{0.56} \cdot K \cdot LS \cdot C \cdot P, \quad (1)$$

where Y is soil losses in tons per a studied period; Q_T is the total volume of discharge in the studied period (m^3); $Q_{\max}$ is the maximum water discharge during the studied period (m^3/s); K is a soil erodibility factor ($h \cdot MJ^{-1} \cdot mm^{-1}$); LS is a dimensionless slope length and gradient factor; C is a dimensionless land management factor; and P is a dimensionless erosion control practice factor (in our case this parameter is equal to 1). The MUSLE approach and its modified versions have been widely applied in different river basins (Williams, 1975; Erskine et al., 2002; Neitsch et al., 2005; Sadeghi et al., 2007).

Soil erodibility factor (K) represents soil loss in t/ha for a particular soil in cultivated, continuous fallow with an arbitrarily selected slope length of 22.13 m and slope steepness of 9%. The K factor is a measure of the susceptibility of soil particles to detachment and transport by rainfall and runoff. The soil texture is the principal factor affecting K, but structure, organic matter and permeability also contribute. According to Unified National Soil Register two soil types were determined: Vulkanicheskie Sloisto-Peplovie and Lahar Soils. From Unified National Soil Register the percentage of clay, silt, sand, and organic matter content was received. The J.R. Williams equation was used (Williams, 1995):

$$K = f_{csand} \times f_{cl-si} \times f_{orgc} \times f_{hisand}, \quad (2)$$

$$f_{csand} = 0.2 + 0.3 \times \exp\left(-0.256 \times m_s \times \left(1 - \frac{m_{silt}}{100}\right)\right), \quad (3)$$

$$f_{cl-si} = \left(\frac{m_{silt}}{m_c + m_{silt}}\right)^{0.3}, \quad (4)$$

$$f_{orgc} = 1 - 0.0256 \times \frac{orgC}{orgC + \exp\left(-5.51 + 22.9 \times \left(1 - \frac{m_s}{100}\right)\right)}, \quad (5)$$

$$f_{hisand} = 1 - \frac{0.7 \times \left(1 - \frac{m_s}{100}\right)}{\left(1 - \frac{m_s}{100}\right) + \exp\left(-5.51 + 22.9 \times \left(1 - \frac{m_s}{100}\right)\right)}, \quad (6)$$

where m_s is sand content, %; m_{silt} is silt content, %; m_c is clay content, %; $orgC$ is organic matter content, %. Therefore for lahar soils the K value is equal to 0.4 $h \cdot MJ^{-1} \cdot mm^{-1}$ and for Vulkanichiskie Sloisto-Peplovie -0.28 $h \cdot MJ^{-1} \cdot mm^{-1}$.

The slope length and gradient factor (LS) was calculated using a formula developed by Mitasova et al. (1996):

$$LS = (m+1) \cdot \left[\frac{Ac}{a_0}\right]^m \cdot \left[\frac{\sin\beta}{b_0}\right]^n, \quad (7)$$

where Ac is upslope contributing area per unit contour width (m), β is the slope in degrees, m and n are dimensionless parameters, a_0 = 22.1 m is the length and $b_0 = 5.16°$ is the slope angle of a standard USLE (Universal Soil Loss Equation) plot. Designations for exponents m and n values can be found in the literature. We omit a detailed discussion here, but readers should refer to Oliveira et al. (2013) and Mitasova et al. (1996) for case studies and examples. It appears that using $m = 0.4$ and $n = 1.6$ is typical. The estimation of the local LS factor was based on digital elevation model (DEM) "ALOS WORLD 3D" with 5-meter resolution.

The land management factor (C) was estimated using a relationship with $NDVI$ (Normalized Difference Vegetation Index, Tweddales et al., 2000):

$$C = \exp\left(-2\frac{NDVI}{1 - NDVI}\right). \quad (8)$$

The local $NDVI$ values were calculated with $NDVI = \frac{NIR - RED}{NIR + RED}$ where NIR are values of near infrared and RED of red spectra of satellite images (Jensen, 2000). The calculation of $NDVI$ for different seasons was carried out using Landsat 7 ETM + for (24.07.2012 and 15.06.2013) and Landsat 8 (for 20.06.2014) satellite images.

2.3.2 Sediment Delivery Calculation

Sediment transport within the catchment was evaluated using the sediment delivery approach:

$$E = \sum\nolimits_i MUSLE_i \cdot SDR_i, \quad (9)$$

where E - sediment export from subcatchments, t/yr; $MUSLE_i$ - the result of Eq. (1), i.e., soil losses in t/ha per period. The calculation of the sediment delivery ratio (SDR) is based on DEM for each ith cell (Borselli et al., 2008):

$$SDR_i = \frac{SDR_{\max}}{1 + \exp\left(\frac{IC_0 - IC_i}{k}\right)}, \quad (10)$$

where $SDR_{\max}$ is the maximum theoretical SDR, set to an average value of 0.8 (Vigiak et al., 2012), and IC_0 and k are calibration parameters equals 0.5 and 2 correspondingly which define the shape of the SDR-IC relationship (increasing function) and; IC_i – connectivity index calculated as:

$$IC = \log_{10}\left(\frac{D_{\text{up}}}{D_{\text{dn}}}\right), \quad (11)$$

where D_{up} is the upslope component (m) defined as $D_{\text{up}} = \overline{CS}\sqrt{A}$ where $\overline{C}$ is the average C factor of the upslope contributing area, $\overline{S}$ is the average slope gradient of the upslope contributing area (m/m) and A is the upslope contributing area (m^2). The upslope contributing area is delineated from the D-infinity flow algorithm (Tarboton, 1997). D_{dn} is the downslope component defined as:

$$D_{\text{dn}} = \sum\nolimits_i \frac{d_i}{C_i S_i}, \quad (12)$$

where d_i is the length of the flow path along the i^{th} cell according to the steepest downslope direction (m), C_i and S_i are the C factor and the slope gradient of the i^{th} cell, respectively. Again, the downslope flow path is determined from the D-infinity flow algorithm (Tarboton, 1997).

Modeling results were compared with measured sediment load at gauging stations:

$$\Delta = \frac{W_{\text{mod}} - W}{W} \cdot 100\%, \quad (13)$$

where Δ - difference between modeling results and observations, %; W_{mod} – modeling assessment of sediment export (tons); W – measurement data, (tons).

The calculation using MUSLE (1) was made for 7 gauging stations (Fig. 1 and Table 1) for 3 time series: august 2012, June 2013, June 2014.

3 Results and discussion

3.1 Field observations of sediment yield fluctuations

During all recorded periods, a diurnal variation of water and sediment flow was clearly visible (Fig. 4). According to the field data July–August 2012 the most significant water discharges (Q) (up to 0.92 m^3/s) were recorded at station No 3 located in the watershed type I covering volcanic slopes. The values of the discharges decreased in the downstream direction within the watershed type II. Despite some contribution from the tributaries located in watershed types III (maximum 0.15 m^3/s and 0.27 m^3/s at

stations No 5 and No 7 respectively) there was no discharge recorded in the most downstream stations No 10B and 11B (Table 1). These discharge losses in the downstream direction were most probably caused by water infiltration into porous deposits of the lahar valley (watershed type II).

Despite the recorded precipitation in July–August 2012 both the distribution of the discharges within the basin and the intra-daily patterns of the observed discharge fluctuations (Fig. 4(a)) imply major water contribution from the temperature triggered melting of the snow patches on the volcanic slopes (watershed type I). The differences in inter-daily fluctuations at different stations (Fig. 4) imply a strong influence of the distribution of water sources and local conditions (e.g., the geology of the lahar valleys). The latter can also have an influence on intra-hourly water level fluctuations in the channels (station No 6, Fig. 4(b)). As could be seen these short-term water level oscillations may occur independently from water discharge and sediment transport fluctuations which provide a evidence to explain it by the role of in-channel processes. Local aggradation/degradation patterns which occur in unstable channel of the lahar valley may cause fast water level changes. The short-term fluctuations could be also induced by rapid filling and release of the shallow underground aquafers of the lahar deposits (intervals of pulsations lasting 5–10 minutes, Fig. 5). Such short-term changes in water and consequently sediment discharges are common within river sections of lahar valleys (Mouri et al., 2014).

The patterns of sediment concentration peaks in 2012 followed the water discharge peaks in most of the cases at all stations. Few water discharge peaks at stations No 3 and No 5 resulted in delayed increase of even constant sediment concentrations. The patterns of water discharge-sediment concentration depend among others on the availability and sources of the transportable sediments during the flow events (Pietroń et al., 2015). The primary sources of sediment in the studied basin are volcanic slopes that feed the fluvial system. Thus, sediment concentrations (*SSC*) up to $5 \cdot 10^3$ mg/L were recorded at the watershed type I at station No 3. These *SSC* values corresponded to sediment loads ($SL = Q \cdot SSC$) up to max 394 t/day (16.6 t/h) and on average 60 t/day. Despite the decreased water discharge between stations No 3 and No 6 the sediment concentrations and loads were still very high (up to $9 \cdot 10^4$ mg/L and 42.1 t/h respectively during the *Q* peaks. The high slopes (25‰–60‰) of the lahar valleys bottom and relatively low weight of the material increases the efficiency to transport the sediments originating from watershed type I further downstream. Thus, the size of transported particles in the watershed type II (station No 6) could reach up to 5 cm even with water discharge of 0.1 m^3/s. Additionally, the rapid *SSC* responses to the water discharge peaks in the watershed type II (station No 6, Fig. 4) could be triggered by remobilization of in-channel material (see Pietroń et al., 2015).

The observations in June–July 2013 and June 2014 represented early summer conditions when the upper part of the catchment was still covered by snow. During both periods of observation constant and relatively steady discharges were recorded at station No 1 (up to 0.1 m^3/s and 1.2 m^3/s in 2013 and 2014, respectively, Table 1 and Fig. 4) located on in watershed type I. This character of water flows could be due to relevant thermal conditions of the volcanic slopes (aspect and sun exposure of the slopes as well as heating from the active volcano) that were causing regular melting of the snow packs. The main parts of the lahar valleys were still filled with a thick snow cover until the end of June–July. The water discharges in the downstream locations within the watershed type II (stations No 6, 10B and 11B, Fig. 4) were more unsteady (irregular) and extremely low (around 0.01 m^3/s). No flow conditions were recorded both in 2013 and 2014 below station No 1 until station No 10B and places located below the retreating snow packs. The length of dry river network reached 10 km.

The sediment transport within the mountain channels (watersheds I and III, stations No 5, 7, 3, 1) during all periods was characterized with small suspended sediment concentration (*SSC)* fluctuations which remained below

Table 1 Subcatchments and recorded flow parameters of Sukhaya Elizovskaya River

Nostation (Fig. 1)	Area/ km^2	Average attitude/m	Average slope/%	Precipitation during observation period/mm			Total runoff depth during observation period/mm			Maximal water discharge during observation period/($m^3 \cdot s^{-1}$)		
				Aug. 2012	June 2013	June 2014	Aug. 2012	June 2013	June 2014	Aug. 2012	June 2013	June 2014
1	1.26	1440	47.2	-*	-	13.5	200	10.1	278.0	1.0	0.1	1.2
3	6.16	1278	45.9	18	-	-	57.1	0	0	0.92	0	0
5	1.94	891	22.6	18	-	-	23.2	20.0	18.7	0.15	0.12	0.11
6	25.2	1255	132	18	6.2	-	1.49	0.53	0	0.10	0.01	0
7	8.33	1262	41.8	18	-	-	12.6	0	0	0.27	0	0
10B	41.5	1144	91.2	0	6.2	-	0	0.02	0	0	0.004	0
11B	49.7	1102	35	0	6.2	-	0	0.04	0	0	0.02	0

* - flow was not recorded

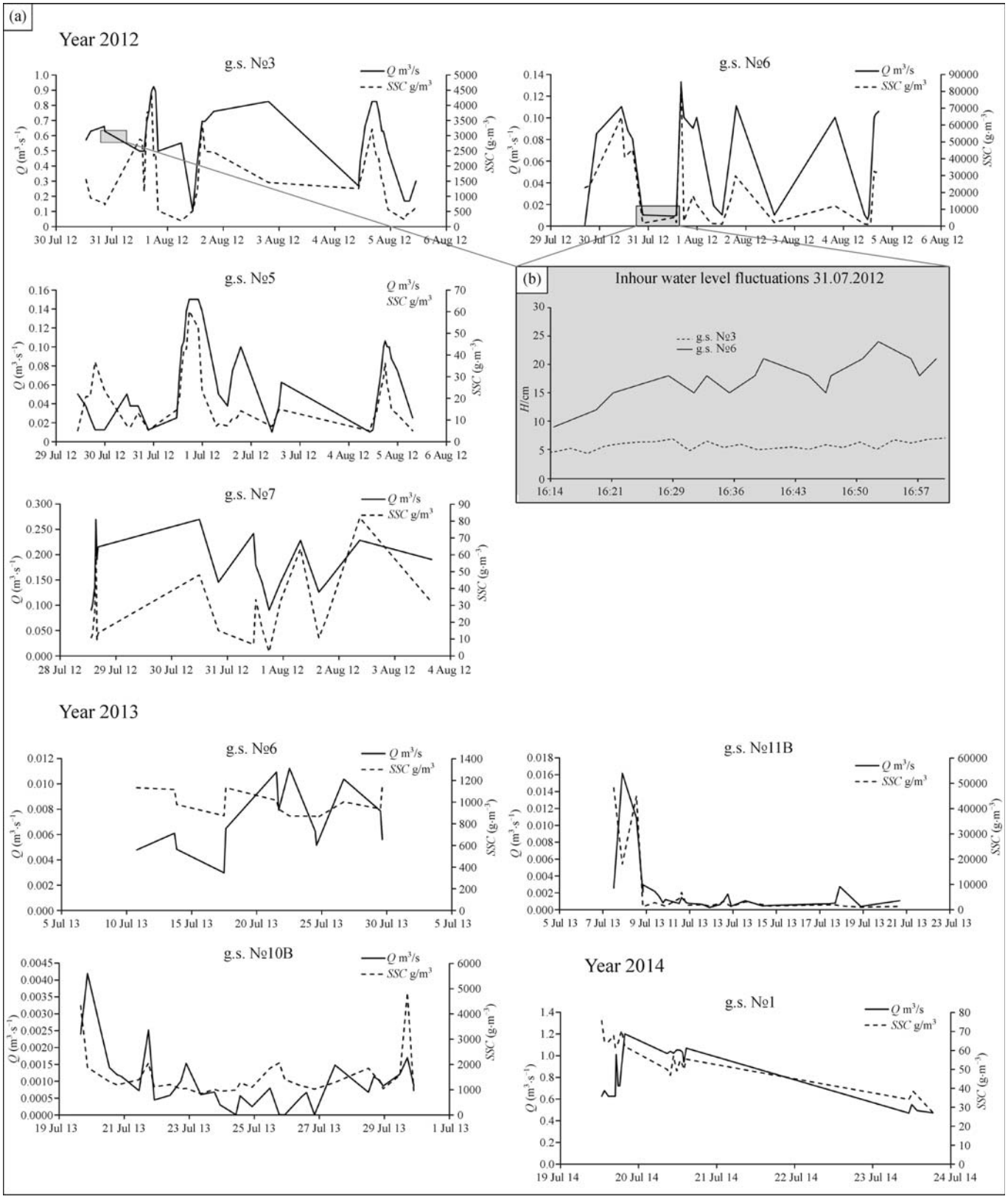

Fig. 4 Spatiotemporal fluctuations of water flow and suspended sediment concentration.

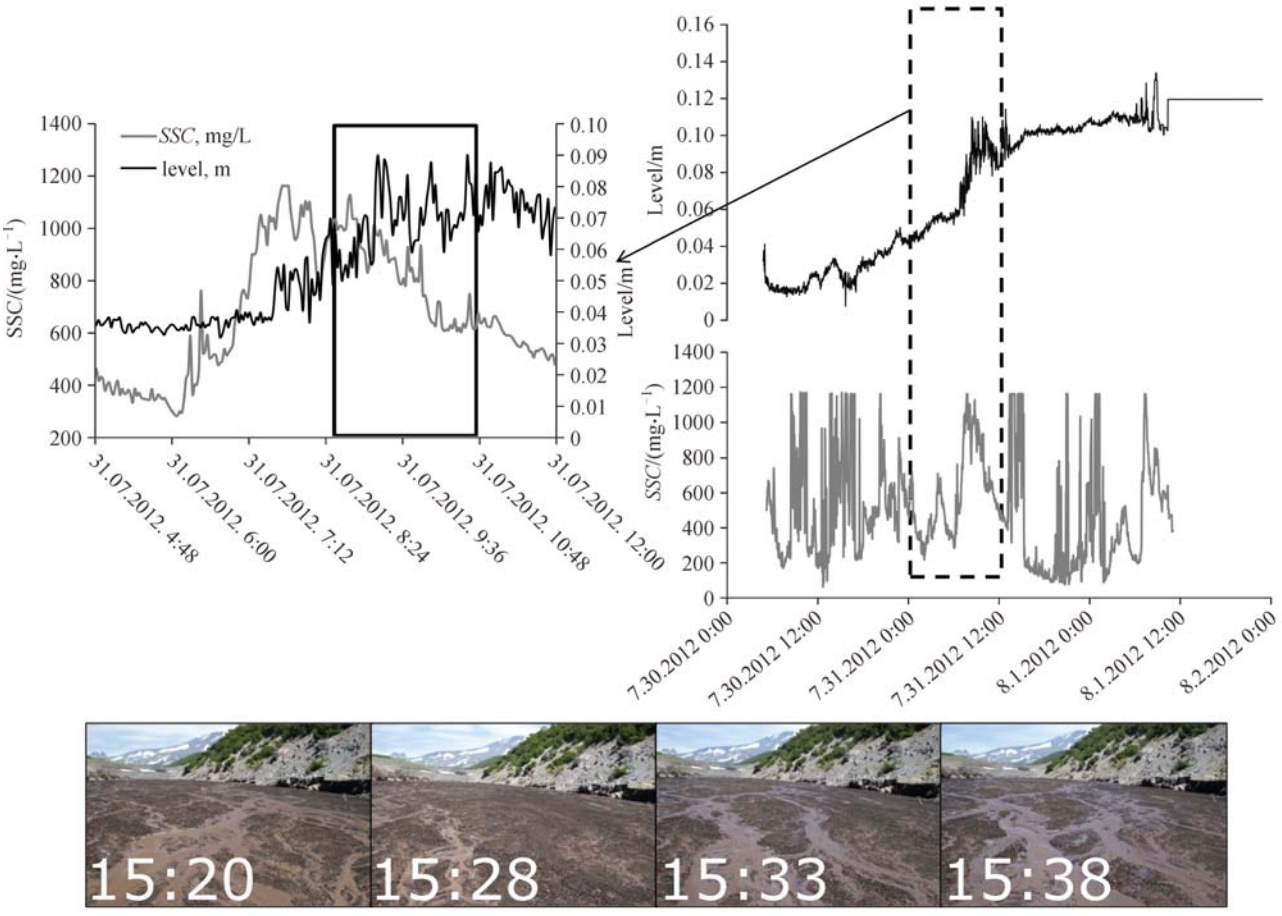

Fig. 5 Short-term fluctuations of water level (level, m) and suspended sediment concentrations (mg/L) (up) and related fast channel changes (down) of the Sukhaya Elizovskya river (summer 2012) (gauging station No 6).

$3 \cdot 10^3$ mg/L during flow events and most often below 100 mg/L in the whole period. The irregularity of water flow at the downstream stations (No 10B and 11B) determined the sediment transport features. The sediment concentration reach almost $6 \cdot 10^4$ mg/L at these locations after a flow water discharge event in July 2013 (Fig. 4), while most *SSC* at station No 11B were below $1 \cdot 10^3$ mg/L.

In June 2014, due to huge amounts of accumulated snow in the lahar valleys, the water and sediment flows entering the valley from the watersheds type I (volcanic slopes) caused development of a phenomena which we called "supranival flow". Rapidly delivered light pyroclastic material formed alluvial armoring layer by depositing vast amounts of sediments on the surface of the snowpack during intensified snow melt events (Fig. 6). The channel was formed on the top of the 4–5 m deep snowpack. The particular length of the flow before it infiltrated into the snow correlates with amount of water entering the river valley from upstream catchment No 1 and thus, representing daily variations of runoff (Fig. 4).

Altogether, the irregularity of sediment yield is determined by the fluctuations of water flow which, in turn, is determined by the inflow volume from the snow packs. Rainfall because of the dominant role of snowmelt and a high rate of filtration does not have a significant impact on water flow within the lahar valley.

Short-term water flow fluctuations are exclusively typical for lahar valleys and have relatively low impact on *SSC*. Such high-frequency water and sediment flow fluctuations are known for glacial river basins (Ballantyne and McCann,1980). It is common (Stott and Grove, 2001) that daily fluctuations vary with snowmelt and precipitation while the more frequent oscillations are determined by the water retention processes in the body of glaciers and snowfields (Ballantyne and McCann,1980). The comparison of these data (Ballantyne and McCann, 1980; Stott and Grove, 2001) with our assessment show similar fluctuation magnitudes of water discharges in the glacial basins that correspond to one order of magnitude less sediment load in respect to volcanic watersheds.

The maximum sediment yield was measured at gauging station No 3 in 2012 (average 60 t/day). Downstream there was a decrease in sediment yield till gauging station No 6. Downstream reaches were dry in this particular period. In

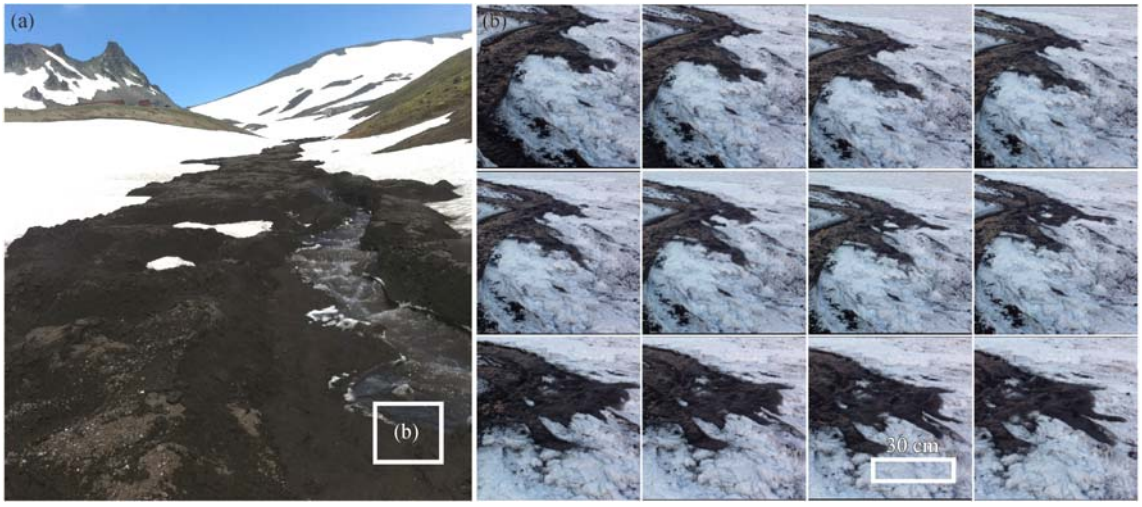

Fig. 6 "Supranival flow" at the top of 4−5 meters depth snowpacks in lahar valleys with an armouring layer of pyroclastic material: (a) upstream view of the lahar valley with a supranival flow; (b) stream's front short-term evolution (photos made every 1 sec) (23 June 2014).

June 2013 and 2014 constant sediment load was observed at gauging stations No 10B and No 11B which were located directly below the retreating snow cover, covering most part of the basin. In this period of the year the maximum value of sediment load was observed in the upper parts of the river network where a constant flow was observed on relatively short sections of the channel. Downstream the flow infiltrates into the lahar deposits under the snow cover.

The presented data show that quick changes in thermal conditions on volcanic slopes can lead to very rapid snowmelt triggered flows of pyroclastic material (e.g., supranival flow in 2014). In principle, larger in scale eruptive and post eruptive rapid debris flows caused by rapidly melting snow cover can have destructive consequences (Waitt, 1989; Pierson et al., 1990; Kilgour et al., 2010).

3.2 Sediment transport modeling

Application of the MUSLE model (Fig. 7) provides an insight on the applicability of numerical erosion models to volcanic catchment. For all hydrological events (June and July–August) at gauging stations No 5, and 7 (III type of watershed) the difference between predicted and observed values was low (percentage error 9.7%). Higher values of error (–273%) were observed in high-relief sub-basins of the watershed type I (Table 2). For all other stations (No 3, 6, 10B, 11B) the percentage error equals to –97%. The low correlation between predicted and observed values for watershed type II suggest a dominant influence of local factors such as low bulk density and high filtration rates of lahar deposits. This indicates the necessity of adjustments of Eqs. (2) and (4) of USLE and MUSLE. The influence of infiltration into the thick lahar deposits on sediment yield determines the need to modify the structure of Eq. (1) using physically based (dynamic) algorithms. It should be pointed out that MUSLE parameters much better characterize the conditions of type III sub-basins.

The results of the sediment transport modeling indicate the maximum sediment yield from type II sub-basins and minimum from type III sub-basins. Longitudinal changes in the water flow within the lahar valleys determine the position of the accumulation zones. For example, mean value of accumulation between stations No 3 and No 6 is 319 ton which correspond to daily deposition of 53 ton/day. With regard to the distance between the stations (4.7 km) the intensity of accumulation can be estimated to an amount of 11.3 ton/day. Using a bulk density value of 1000 kg/m^3 (Tanarro et al., 2010) and a valley width value of 30 m the average accumulation layer value was estimated to 7.2 mm for the 3 summer months. It is important to mention that both modeled and observed values relates to total (bed and suspended) sediment transport. This is particularly important for the lahar valley channels where due to hyperconcentrated flow even coarse particles (sand and gravel) could be transported in suspension.

Comparison between observed (Table 2) and modeled values demonstrate main constraints and perspectives of the modeling efforts to study sediment transport in volcanic area. The MUSLE approach has been applied to a wide range of different catchments and has often delivered satisfactory estimates of storm based sediment yields (Erskine et al., 2002; Blaszczynski, 2003). However, in some cases the model can over or under predict the sediment yields when compared with observed values due to, for instance, lack of data representing anthropogenic impacts (Jaramillo, 2007; Chandramohan et al., 2015) or

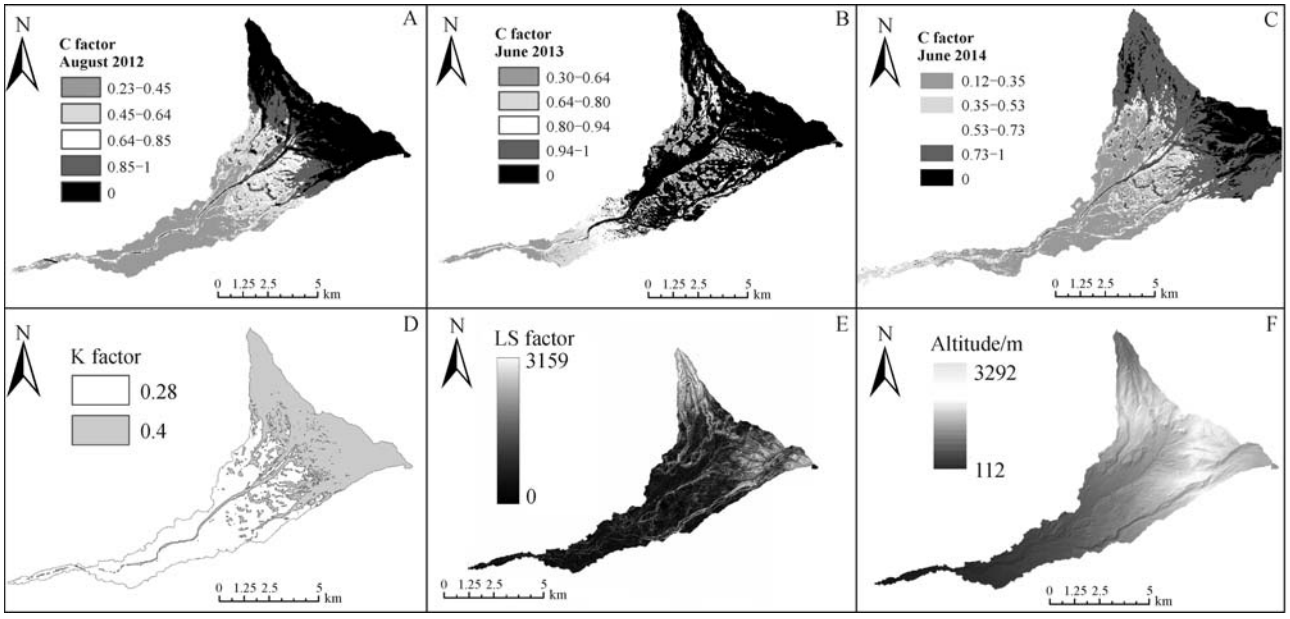

Fig. 7 MUSLE model parameters.

Table 2 Modeled and observed values of sediment transport of Sukhaya Elizovskaya River

Catchment type	No station (Fig. 1)	Measured values			Modeled values (MUSLE)		
		29.07–5.08 2012	7.06–30.06 2013	19–24.06 2014	29.07–5.08 2012	7.06–30.06 2013	19–24.06 2014
I	1	8.7	2.1	12.6	-	-	47.1
II	3	440	0	0	25.7	-	-
III	5	0.57	0.5	0.46	0.5	-	-
II	6	106	84.8	0	3.73	2.63	-
III	7	2.32	0	0	2.19	-	-
II	10B	0	1.2	0	-	0.04	-
II	11B	0	36.1	0	-	1.03	-

misrepresentation of the physical characteristic of the studied basins (Sadeghi et al., 2014). Additionally, since the MUSLE model was developed for storm events and specific river basin conditions lack of calibration or use in areas with divergent physical properties, such as river basins characterized with unconsolidated sediments and high sediment yields (e.g., badlands in Spain; Appel et al., 2006) can result in significant errors. In this study, the calibrated model results for non lahar watersheds (type III) were satisfactory. However, the modelling of the volcanic slopes and lahar valleys watersheds (type I and II) resulted in high errors.

Additional errors raised from *LS* factor estimates due to unpredictable high slope gradients – sometimes it can be more than 45 degrees. Presumable, the fluctuating and heterogeneous infiltration patterns within these watersheds modify the flow conditions and make a unique features of MUSLE. According to our search in ISI Web of Knowledge and Google Scholar no results of the MUSLE approach from lahar valleys or snow melt dominated areas has been published before. However, effective predictions of rapid and often destructive sediment flows in lahar river basins are needed (Carranza and Castro, 2006). Hence, relevant modifications of the MUSLE model for the lahar river basins can aid in better predictions of snowmelt triggered sediment flow events and improve risk management and mitigation strategies.

4 Conclusions

1) The seasonal and daily water regime of the rivers draining from the volcanoes through lahar valleys is driven by distribution of snow within the catchment. Year to year the water discharge at the same place at the same period may differ from 0.001 m^3/s to 1–2 m^3/s. On the other hand the high-speed channel changes due to the high erodibility of volcanic and lahar deposits have an effect on water flow.

The infiltration characteristics of the deposits have a high impact on underground flow which in turn governs intra-hourly fluctuations.

2) Lahar valley rivers perform extreme values of sediment load. Diurnal fluctuations of sediment load may reach up to $9 \cdot 10^4$ mg/L which corresponds to an increase of two orders of magnitude during a day. Against this background the invariant accumulation (~1 cm/year) at the valley bottoms happens even during the low-flow periods but during lahar events this rates may increase to several meters per year.

3) The adjustment of the Modified Universal Soil Loss Equation delivered acceptable results when compared to the observed values for the conditions of volcanic regions located outside from lahar watersheds (type II). None of parametric models (like MUSLE etc.) are relevant to describe extremely complicated sediment transport within the lahar valleys, especially in case of such phenomena like supranival flows. At the same time we assume that the slope wash in this volcanic catchment has a significant control over the whole sediment patterns. Following this assumption on the catchment scale adequate estimates of MUSLE parameters could provide reliable data on general sediment transport – one of the main outputs of this study. However, further sediment modeling in lahar valleys should take into account diurnal and sub-hourly fluctuations of water flow and high filtration rates in lahar deposits.

Acknowledgements This research was conducted within the project of Russian Scientific Foundation No 14-27-00083. The field research was additionally funded by the following projects: Russian Fund for Basic research project No 15-05-05515, 16-55-53116 and 16-35-00567; PEOPLE MARIE CURIE ACTIONS International Research Staff Exchange Scheme Call: FP7-PEOPLE-2012-IRSES *Fluvial processes and sediment dynamics of slope channel systems: Impacts of socio economic-and climate change on river system characteristics and related services*. The Swedish partners were funded from the Swedish Research Council Formas (project 2012-790). We thank all participants of the field work in 2012–2014 and especially are grateful to Simone Mori who designed Fig. 2.

References

Alexeevsky N I, Chalov R S, Berkovich K M, Chalov S R (2013). Channel changes in largest Russian rivers: natural and anthropogenic effects. International Journal of River Basin Management, 11(2): 175–191

Appel K, Mueller E N, Francke T, Opp C (2006). Soil-erosion modelling along badland hillslopes in a dryland environment of NE Spain. Geophys Res Abstr, 8: 02874

Ballantyne C K, McCann S B (1980). Short-lived damming of a high-Arctic ice-marginal stream, Ellesmere Island, N. W. T., Canada. J Glaciol, 25: 487–491

Blaszczynski J (2003). Estimating watershed runoff and sediment yield using a GIS interface to curve number and MUSLE models. Soils and Geology, Resources Notes No. 66, National Science and Technology Center, Denver

Boardman J (1996). Soil erosion by water: problems and prospects for research. In: Anderson M G, Brooks S M, eds. Advances in Hillslope Processes. Chichester: Wiley, 489–505

Bøggild C E (2000). Preferential flow and melt water retention in cold snow packs in West-Greenland. Hydrol Res, 31(4–5): 287–300

Borselli L, Cassi P, Torri D (2008). Prolegomena to sediment and flow connectivity in the landscape: a GIS and field numerical assessment. Catena, 75: 268–277

Carranza E J M, Castro O T (2006). Predicting lahar-inundation zones: case study in West Mount Pinatubo, Philippines. Nat Hazards, 37(3): 331–372

Chalov S R, Leman V N, Chalova A S (2014). In-channel processes hazards and salmon habitats at the Kamchatka Peninsula. Moscow: VNIRO (in Russian)

Chandramohan T, Venkatesh B, Balchand A N (2015). Evaluation of three soil erosion models for small watersheds. Aquatic Procedia, 4: 1227–1234

Cronin S J, Neall V E, Lecointre J A, Palmer A S (1999). Dynamic interactions between lahars and stream flow: a case study from Ruapehu volcano, New Zealand. Geol Soc Am Bull, 111(1): 28–38

Doyle E E, Cronin S J, Thouret J C (2011). Defining conditions for bulking and debulking in lahars. Geol Soc Am Bull, 123(7–8): 1234–1246

Eiriksdottir E S, Louvat P, Gislason S R, Óskarsson N, Hardardóttir J (2008). Temporal variation of chemical and mechanical weathering in NE Iceland: evaluation of a steady-state model of erosion. Earth Planet Sci Lett, 272(1–2): 78–88

Ermakova A S (2008). Correspondence of longitudinal profiles and vertical riverbed deformations with the riverbed types on the Kamchatka Peninsula. Geomorphology RAS, 4: 65–74 (in Russian)

Erskine W D, Mahmoudzadeh A, Myers C (2002). Land use effects on sediment yields and soil loss rates in small basins of Triassic sandstone near Sydney, NSW, Australia. Catena, 49(4): 271–287

Gerdel R W (1954). The transmission of water through snow. Eos (Wash DC), 35(3): 475–485

Gran K B, Montgomery D R (2005). Spatial and temporal patterns in fluvial recovery following volcanic eruptions: channel response to basin-wide sediment loading at Mount Pinatubo, Philippines. Geol Soc Am Bull, 117(1): 195–211

Hayes S K, Montgomery D R, Newhall C G (2002). Fluvial sediment transport and deposition following the 1991 eruption of Mount Pinatubo. Geomorphology, 45(3–4): 211–224

Hock R (1999). A distributed temperature-index ice-and snowmelt model including potential direct solar radiation. J Glaciol, 45(149): 101–111

Jaramillo F (2007). Estimating and modeling soil loss and sediment yield in the Maracas-St. Joseph River Catchment with empirical models (RUSLE and MUSLE) and a physically based model (Erosion 3D). Thesis (MSc), Civil and Environmental Engineering Department, McGill University, Montreal

Jensen J R (2000). Remote Sensing of the Environment: An Earth Resource Perspective. New Jersey: Prentice Hall

Kilgour G, Manville V, Della Pasqua F, Graettinger A, Hodgson K A, Jolly G E (2010). The 25 September 2007 eruption of Mount Ruapehu, New Zealand: directed ballistics, surtseyan jets, and ice-

slurry lahars. J Volcanol Geotherm Res, 191(1): 1–14

Kuksina L V, Chalov S R (2012). The suspended sediment discharge of the rivers running along territories of contemporary volcanism in Kamchatka. Geogr Nat Resour, 33(1): 67–73 (English Translation of Geografiya I Prirodnye Resursy)

Lavigne F, Thouret J C, Voight B, Suwa H, Sumaryono A (2000). Lahars at Merapi volcano, Central Java: an overview. J Volcanol Geotherm Res, 100(1–4): 423–456

Major J J, Pierson T C, Dinehart R L, Costa J E (2000). Sediment yield following severe volcanic disturbance – A two-decade perspective from Mount St. Helens. Geology, 28(9): 819–822

Manville V, Hodgson K A, Houghton B F, Key J R H, White J D L (2000). Tephra, snow and water: complex sedimentary responses at an active snow-capped stratovolcano, Ruapehu, New Zealand. Bull Volcanol, 62(4–5): 278–293

Marenina T U, Sirin A N, Timerbaeva K M (1962). Koryakskii volcano on Kamchatka Peninsula. Proc. Lab. Volcanology. 1962. No 22. P. 67–130

Mitasova H, Hofierka J, Zlocha M, Iverson L R (1996). Modelling topographic potential for erosion and deposition using GIS. International Journal of Geographical Information Systems, 10(5): 629–641

Mouri G, Ros C F, Chalov S R (2014). Characteristics of suspended sediment and river discharge during the beginning of snowmelt in volcanically active mountainous environment. Geomorphology, 213: 266–276

Neitsch S L, Arnold J G, Kiniry J R, Williams J R, King K W (2005). SWAT theoretical documentation. Soil and Water Research Laboratory: Grassland, 494: 234–235

Oguchi T, Saito K, Kadomura H, Grossman M (2001). Fluvial geomorphology and paleohydrology in Japan. Geomorphology, 39 (1–2): 3–19

Oliveira A H, da Silva M A, Silva M L N, Curi N, Neto G K, de Freitas D A F (2013). Development of topographic factor modeling for application in soil erosion models. In: Soriano M C H, ed. Soil Processes and Current Trends in Quality Assessment. InTech, 111–138

Pellerin B A, Saraceno J F, Shanley J B, Sebestyen S D, Aiken G R, Wollheim W M, Bergamaschi B A (2012). Taking the pulse of snowmelt: in situ sensors reveal seasonal, event and diurnal patterns of nitrate and dissolved organic matter variability in an upland forest stream. Biogeochemistry, 108(1–3): 183–198

Pierson T C, Janda R J, Thouret J C, Borrero C A (1990). Perturbation and melting of snow and ice by the 13 November 1985 eruption of Nevado del Ruiz, Colombia, and consequent mobilization, flow and deposition of lahars. J Volcanol Geotherm Res, 41(1): 17–66

Pietroń J, Jarsjö J, Romanchenko A O, Chalov S R (2015). Model analyses of the contribution of in-channel processes to sediment concentration hysteresis loops. J Hydrol (Amst), 527: 576–589

Ponomareva V, Melekestsev I, Braitseva O, Churikova T, Pevzner M, Sulerzhitsky L (2007). Late Pleistocene–Holocene Volcanism on the Kamchatka Peninsula, Northwest Pacific Region. In: Eichelberger J, Gordeev E, Izbekov P, Kasahara M, Lees J, eds. Volcanism and Subduction: The Kamchatka Region. Washington D.C.: American Geophysical Union, 165–198

Rad S D, Allègre C J, Louvat P (2007). Hidden erosion on volcanic islands. Earth Planet Sci Lett, 262(1–2): 109–124

Renard K G, Foster G R, Weesies G A, McCool D K, Yoder D C (1997). Predicting Rainfall Erosion Losses—A Guide to Conservation Planning with the Revised Universal Soil Loss Equation (RUSLE). U.S. Dept. Agriculture, Agricultural Handbook 703, Washington, DC

Rodolfo K S, Arguden A T (1991). Rain-lahar generation and sediment-delifery systems at Mayon volcano, Philippines. In: Fisher R V, Smith G A, eds. Sedimentation in Volcanic Settings. Society for Sedimentary Geology, Tulsa: SEPM Special Publication 45, 59–70

Sadeghi S H R, Gholami L, Khaledi Darvishan A, Saeidi P (2014). A review of the application of the MUSLE model worldwide. Hydrol Sci J, 59(2): 365–375

Sadeghi S H R, Mizuyama T, Miyata S, Gomi T, Kosugi K, Mizugaki S, Onda Y (2007). Is MUSLE apt to small steeply reforested watershed? J For Res, 12(4): 270–277

Smith G A, Fritz W J (1989). Volcanic influence on terrestrial sedimentation. Geology, 17(4): 375–376

Smith G A, Lowe D R (1991). Lahars: Volcano-hydrologic events and deposition in the debris flow – hyperconcentrated flow continuum. In: Fisher R V, Smith G A, eds. Sedimentation in Volcanic Settings. Society for Sedimentary Geology, Tulsa: SEPM Special Publication 45, 59–70

Stott T A, Grove J R (2001). Short-term discharge and suspended sediment fluctuations in the proglacial Skeldal River, nort-east Greenland. Hydrol Processes, 15(3): 407–423

Sun X, Rosin P L, Martin R R, Langbein F C (2007). Fast and effective feature-preserving mesh denoising. IEEE Trans Vis Comput Graph, 13(5): 925–938

Tanarro L M, Andrés N, Zamorano J J, Palacios D, Renschler C S (2010). Geomorphological evolution of a fluvial channel after primary lahar deposition: Huiloac Gorge, Popocatépetl volcano (Mexico). Geomorphology, 122(1–2): 178–190

Tarboton D (1997). A new method for the determination of flow directions and upslope areas in grid digital elevation models. Water Resour Res, 33(2): 309–319

Thouret J C, Oehler J F, Gupta A, Solikhin A, Procter J N (2014). Erosion and aggradation on persistently active volcanoes—A case study from Semeru Volcano, Indonesia. Bull Volcanol, 76(10): 857

Tweddales S C, Eschlaeger C R, Seybold W F (2000). An Improved Method for Spatial Extrapolation of Vegetative Cover Estimates (USLE/RUSLE C factor) using LCTA and Remotely sensed imagery. Champaign: Construction Engineering Research Laboratory

Vigiak O, Borselli L, Newham L T H, Mcinnes J, Roberts A M (2012). Comparison of conceptual landscape metrics to define hillslope-scale sediment delivery ratio. Geomorphology, 138(1): 74–88

Waitt R B (1989). Swift snowmelt and floods (lahars) caused by great pyroclastic surge at Mount St Helens volcano, Washington, 18 May 1980. Bull Volcanol, 52(2): 138–157

Wang L, Liu H (2006). An efficient method for identifying and filling surface depressions in digital elevation models for hydrologic analysis and modelling. Int J Geogr Inf Sci, 20(2): 193–213

Williams J R (1975). Sediment-yield prediction with universal equation using runoff energy factor. Present and Prospective Technology for Predicting Sediment Yield and Sources, ARS., S-40: 244–252

Williams J R (1995). The EPIC model: Chapter 25. In: Sing V P, ed. Computer Model of Watershed Hydrology. Highlands Ranch: Water

Resources Publications, 909–1000

Wischmeier W H, Smith D D (1960). A universal soil-loss equation to guide conservation farm planning. Trans Int Congr Soil Sci, 7: 418–425

Wischmeier W H, Smith D D (1978). Predicting Rainfall Erosion Losses – A Guide to Conservation Planning. Agricultural Handbook 537, Washington D.C.: U.S. Dept. of Agriculture Unified National Soil Register http://atlas.mcx.ru/